

Comparative Performance Evaluation of VLC, LTE and WLAN Technologies in Indoor Environments

Arooba Zeshan*, Mehdi Karbalayghareh[†], Farshad Miramirkhani[‡], Murat Uysal[§], Tuncer Baykas[¶]

*Department of Electrical and Electronics Engineering Istanbul Medipol University, Turkey

[†]Department of Electrical and Computer Engineering, the University of Texas at Dallas, USA

[‡]Department of Electrical and Electronics Engineering, Isik University, Turkey

[§]Department of Electrical and Electronics Engineering, Özyeğin University, Turkey

[¶]Department of Electrical-Electronics Engineering, Kadir Has University, Turkey

Abstract—Recent years have seen an exponential rise in the demand for indoor wireless connections that have driven future generation networks to aim for higher data rates with extended coverage and affordable rates. The two most prominent technologies for providing indoor wireless connections, WLAN and LTE, have their limitations and they can not coexist in a single band to form heterogeneous networks (HetNets). Visible light communication (VLC) has seen rapid growth in recent years as it has the capability to seamlessly merge with the existing technologies and provide wireless connections with high data rates. VLC based hybrid indoor network effectively combines the preferences of an end-user with the practicality of implementation. In this work, we investigate specific VLC/WLAN and VLC/LTE hybrid scenarios to perform a detailed analysis on the effect of user mobility on the performance of the system and how the performance of the network (in terms of throughput) can be maximized. The study aims to show how different technologies complement each other in the best and even the worst-case scenarios.

Index Terms—Visible light communication, heterogeneous networks, LTE, WLAN, femtocells

I. INTRODUCTION

Indoor data traffic has seen exponential growth over the past few decades. It has been noted that approximately 80% of the data traffic is generated in the indoor environment. According to CISCO's visual network index (VNI) forecast, this number is expected to increase to 96% once the 5G gets deployed [1]. This has motivated researchers all around the globe to try and cater to this increasing traffic demand.

The most important indoor RF-based wireless network, in terms of data traffic volumes and pervasiveness, is the IEEE 802.11-based WLAN system. WLAN has received massive attention from the users but due to the rising demand, it is suffering from a limited spectrum and bandwidth shortage. There are certain limitations in its deployment because of the electromagnetic interference and, therefore, can not be deployed in sensitive areas, such as hospitals, airplanes, mines, etc. To cater to the increased demand and deployment issues data coverage extension becomes a critical subject.

The conventional mobile radio network has also been striving to overcome bandwidth limitations and coverage issues in indoor scenarios. Third Generation Partnership Project (3GPP) standards group has been investigating small cell deployment in Long Term Evolution (LTE) for an increased performance [2]. Femtocell base stations (FBSs), also known as home base stations, and picocells are small cells belonging to the family of low power nodes (LPNs) that fulfill the same function of emulating a cellular base station but are designed to be installed inside a building. The prime difference between these two product families is the cost, capacity, and comparative RF range. FBSs have a short transmit/receive distance and can be readily installed by the user. Picocells have a larger coverage radius and are comparatively much more expensive than FBSs, that is why they are better suited in outdoor scenarios or large enterprises. However, for this work, we have considered FBSs, which are appropriate for small offices and home environments.

In this work, we have performed a comparative analysis between WLAN, VLC, and LTE FBS that contributes towards the extension of coverage in indoor scenarios. Our study aims to highlight the benefits and shortcomings of the three technologies and to lay the groundwork of how heterogeneous systems can be developed to achieve the best possible performance. To the best of our knowledge, no such study has been reported where simultaneous operation and assessment in terms of data rates and coverage, of the three aforementioned technologies have been carried out.

The remaining part of the paper is organized as follows: we present the system model in Section II. In Section III, a detailed, case-specific, comparative analysis is given between the three technologies. The concluding remarks are presented in Section IV.

II. RELATED WORK

Visible light communication (VLC) has emerged as a promising technology for wireless communication in indoor applications due to the inherent advantages, such as higher capacity, larger bandwidth, high security, etc. But along

with these advantages, there are certain shortcomings as VLC establishes a line of sight (LoS) link and can be easily disrupted, also the hardware implementation for the uplink transmission has size limitations. An appropriate solution, therefore, is to combine different technologies and form a heterogeneous network.

Several works in the literature combine RF and VLC [3, 4, 5] while considering different performance criteria such as energy consumption, cost, and handover, etc. It was shown by the authors of [5] that the heterogeneous network outperforms the homogeneous network in terms of coverage and is also energy-efficient. In [4] the authors demonstrated from simulations that the VLC based network performs much better than WLAN IEEE802.11ac in different indoor scenarios i.e., home, small office with cubicles, and open office environment.

Efforts have been done to form a hybrid VLC/LTE network as well. In [6] a water-filling-iteration-extremum (WFIE) is used as a joint resource management strategy that improved the overall system throughput by 59.23%. The authors of [7] proposed a prediction-based handover technique between VLC and LTE that reduced the delay per interruption by an average of 36.5% as compared to other handover techniques.

III. SYSTEM MODEL

In this section, we present the system models of each technology and how they are configured for this study.

A. VLC System Model

For the VLC system model, we have considered a room with dimensions $6\text{ m} \times 6\text{ m} \times 3\text{ m}$, with plaster ceiling/walls and pinewood floor. To investigate the achievable data rates at different locations, the room has been partitioned into 100 cells with an equidistant spacing of 0.6 m in x and y directions, as illustrated in Figure 1. The end user is considered to be standing in the middle of the cell.

We adopt the ray tracing channel modeling approach [8]. Nine luminaries on the ceiling with equidistance spacing is assumed. These are commercially available light-emitting diodes (LEDs) (Cree® CR6-800L) with a 40° half viewing angle. The optical power for each luminary is 11 Watts. This yields an average illumination level of 153 lux which satisfies typical illumination levels for the home environment. The human body is modeled as a CAD object with absorbing property, as shown in Figure 2 (a). The cell phone has a size of $5.5\text{ cm} \times 10.5\text{ cm} \times 0.5\text{ cm}$ and is equipped with multiple photodetectors. The field of view (FOV) and the area of each detector are 85° and 1 cm^2 , respectively. A user with a height of 1.8 m is considered. The user holds the phone in his hand next to his ear with 45° rotation upward the ceiling and at a height of 1.65 m . The channel parameters used in the simulations are given in Table I. Locations for the photodetectors are denoted as D_n , $n = 1, 2, 3 \dots 7$. D_1, \dots, D_5 are placed on the top edge

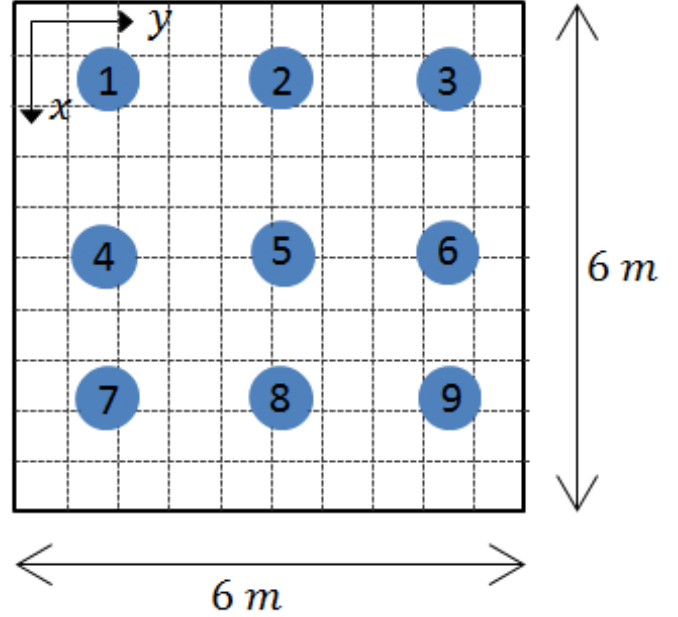


Fig. 1: Illustration of the considered room, where the luminaries are shown as blue circles. The end-user is assumed to be in the center of a cell as she walks around the 100 cells.

TABLE I: Channel parameters for VLC simulations

Room size	$6\text{ m} \times 6\text{ m} \times 3\text{ m}$
Materials	Walls: Plaster Ceiling: Plaster Floor: Pinewood
Objects specifications	Cell phone: Black gloss paint Human body: Absorbing
Luminaire specifications	Number of luminaires: 9 Brand: Cree® CR6-800L Half viewing angle: 40° Power per each luminaire: 11 W
Receiver specifications	Receiver area: 1 cm^2 , FOV: 85°

of the cell phone while D_6 and D_7 are placed on the top two round corners of the cell phone, as can be seen in Figure 2 (b). We consider adaptive direct current biased optical orthogonal frequency division multiplexing (DCO-OFDM) which assigns data to all odd and even subcarriers as:

$$\mathbf{X} = [0 \quad x_1 \quad \dots \quad x_{N/2-1} \quad 0 \quad x_{N/2-1}^* \quad \dots \quad x_1^*] \quad (1)$$

where $n = 0, 1, 2 \dots N-1$ is the number of subcarriers, an N -point inverse fast Fourier transformation (N-IFFT) is applied on \mathbf{X} , which results in a real valued waveform x at the output whose n th element is given by:

$$x[n] = \frac{1}{\sqrt{N}} \sum_{k=0}^{N-1} X[k] e^{2jnkn\pi/N} \quad (2)$$

where $n = 0, 1, 2 \dots N-1$ and $X[k]$ is the modulation symbol that is drawn from 2-PSK and M-QAM with $M = 4, 8, 16, 32, 64, 128$ and 256 . To avoid inter-symbol interference (ISI), a cyclic prefix, of length N_{cp} is further added at the beginning of $x[n]$.

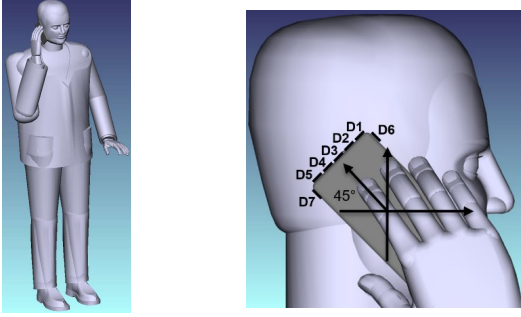


Fig. 2: (left) Human model and (right) location and rotation of PDs on the cell phone

To achieve the unipolar constraint of IM/DD, the waveform is biased with a DC offset (A_{DC}). The resulting time domain waveform is then given as:

$$x(t) = \sum_{n=0}^{N+N_{cp}-1} x[n]\delta(t - nT_s) + A_{DC} \quad (3)$$

where T_s is the sampling interval.

At the receiver's end the signal $y(t)$ is defined as (4).

$$y(t) = R\sqrt{P_x}x(t) \otimes h(t) + n(t) \quad (4)$$

where R is the responsivity of the photodetector (A/W), P_x is the total electrical power, $h(t)$ is the channel impulse response and $n(t)$ is the additive white Gaussian noise (AWGN) with zero mean and variance of σ_N^2 .

Series to parallel operation is performed on the received signal and the CP is removed. The fast Fourier transform (FFT) gives the complex valued symbols in frequency domain. The signal at the k^{th} sub-carrier is now given as:

$$Y[k] = R\sqrt{P_x}X[k]H[k] + N[k] \quad (5)$$

The receiver selects the photodetector which gives the highest data rate while satisfying a target bit error rate (BER). The data rate (in bits per second) is given as:

$$DataRate = \frac{1}{T_s} \frac{N/2 - 1}{L} \log_2 M \quad (6)$$

where $L = N + N_{cp}$ is the total length of the OFDM symbol. The PHY parameters used to simulate VLC are given in Table II. The data rates achieved by the end user is given in Figure 3. The data rates follow a sinusoidal pattern in x and y directions as the maximum data rate is obtained by the photodetector which has the highest channel gain. The achieved minimum and maximum data rates are 23.83 Mbps and 190.67 Mbps, respectively, while an average of 125.36 Mbps is achieved.

B. WLAN System Model

The 802.11-based WLAN networks are one of the widely studied wireless infrastructure for indoor internet access. Indoor signal propagation has been intensively investigated

TABLE II: PHY parameters for VLC simulations

Number of subcarrier	1024
Cyclic prefix length	48
LED turn-on voltage level	2.75 V
LED max-allowed voltage level	4 V
DC bias voltage	3.375 V
Responsivity of PD	1 A/W
Electrical transmit power	0 dBm
Power spectral density of noise	10^{-22} W/Hz
Sampling interval	20 ns
Front-end Bandwidth	20 MHz

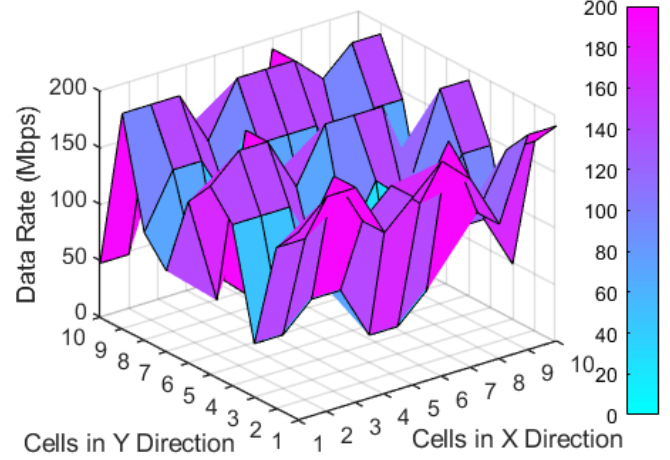


Fig. 3: Data rates achieved as the user walks through the 100 cells within the specified room

over the past years [9, 10, 11, 12]. Typically, the received power (P_{wr}) from the AP to an end user is given as:

$$P_{wr}(d) = \mu_{rss}(d) + S(\sigma, d) \quad (7)$$

where d is the distance between the AP and the user, $\mu_{rss}(d)$ is the average received signal strength and is related to the path loss $P_L(d)$ as $\mu_{rss}(d) = \kappa - P_L(d)$. κ , here, includes transmitted power and transmitting/receiving antenna gain. $S(\sigma, d)$ represents shadowing effect, modelled as a Gaussian random variable with standard deviation σ_n . The path-loss model that incorporates losses due to walls and floors is given as [13] :

$$P_L(d) = PL_o + 10 \times n \times \log_{10}(d) + F_{wall} + F_{floor} \quad (8)$$

In Equation (8), PL_o represents the path-loss in the range of 1 m in free space, n represents loss factor, F_{wall} represents the correction factor of the signal attenuation caused by walls and F_{floor} compensates the signal attenuation caused by floor. For our study we have used Cisco 802.11n WLAN router with the specifications given in Table III. The router uses 802.11n MAC protocol which employs a Carrier Sense Multiple Access with Collision Avoidance (CSMA/CA) method, and supports adaptive modulation with 2-PSK and M-QAM, $M=4, 16, 64$ and 256, coupled with convolutional coding.

TABLE III: Specifications of WLAN and LTE access points

Parameters	WLAN	LTE
Operating frequency	5 GHz	2 GHz
Coverage range	50 m	30 m
Transmit power	23 dBm	20 dBm
Receiver sensitivity	-93 dBm	-62 dBm
Channel bandwidth	20 MHz	20 Mhz
Number of subcarrier	56	1200
Cyclic prefix length	8	144

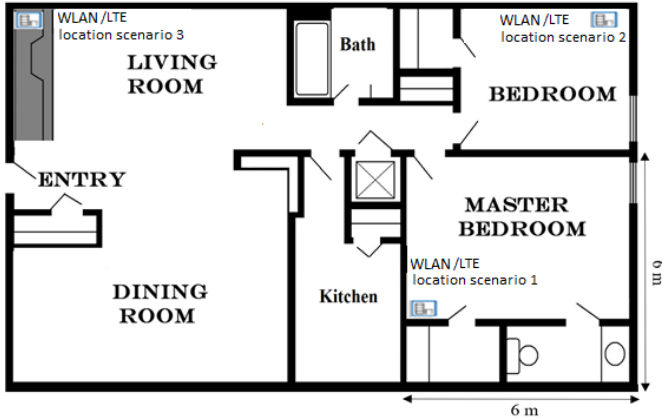


Fig. 4: Layout of the indoor environment under consideration

To form the VLC/WLAN heterogeneous network, we have considered an apartment building with dimensions $10\text{ m} \times 15\text{ m} \times 3\text{ m}$ as illustrated in Figure 4. The simulations of WLAN and LTE FBSs are done in Cisco Packet Tracer. Packet Tracer is free software, provided by Cisco Systems, that allows users to create different network topologies by using routers, switches, and other network devices for the performance evaluation of wireless networks.

The user is assumed to be in the specified room of dimensions $6\text{ m} \times 6\text{ m} \times 3\text{ m}$ (i.e., the same size considered in VLC simulations and labeled as “master bedroom” in Figure 4), the three possible locations of the WLAN router has also been highlighted.

C. LTE System Model

FBSs aims to enhance the coverage provided by the mobile operator’s network by connecting the network to mobile terminals via DSL, cable broadband connections, or optical fibers. In principle, FBS, analogous to a WLAN access point, is a low-cost, low-power wireless carrier base station that is connected directly to the internet and is linked to the carrier cloud [14, 15].

Despite having similar features as that of a WLAN access point, certain benefits make the technology stand out. FBSs are more reliable as they allow a seamless connection between the home network and the main cellular network and thus guarantee a high quality of service. They use

licensed spectrum and, therefore, become less susceptible to random radio interference and assure a more secure transmission. The aforementioned advantages make FBS a good candidate for providing coverage in indoor environments.

The placement of FBSs can further enhance the coverage as a wrongly placed access point could lead to a leakage of signal and burden the core network. Therefore, the transmit power of FBS and the antenna pattern of the macro base station must adhere to certain requirements [16], an estimate of which can be obtained from the following equation:

$$P_{femto,pilot} = \min(P_{macro,pilot} + G_{macro} - L_{macro} + L_{femto}(r), P_{pilot,max}) \quad (9)$$

where, $P_{femto,pilot}$ is the appropriate femtocell pilot power, $P_{macro,pilot}$ is the pilot power transmitted by the macrocell, G_{macro} is macrocell antenna gain in direction of the FBSs, L_{macro} denotes the path loss between the macrocell and the femtocell $L_{femto}(r)$ is the estimated path loss from the femtocell to a device inside radius r . Equation (9) provides a rough estimate of the constant cell range independent of the distance to the macrocell. To highlight the importance of LTE FBS placement, we varied its position to constitute three different scenarios.

For the simulations of LTE FBS, we used the Cisco Small Cell Series. The specifications of FBS that were used in the simulations are given in Table III. The LTE uses radio resource control (RRC) based MAC protocol and supports adaptive modulation with convolutional coding. We further our investigation by recreating the same simulation environment, but this time with LTE FBS, as shown in Figure 4 and assess its performance as opposed to the performance of VLC.

IV. COMPARATIVE ANALYSIS OF COVERAGE AND DATA RATE

In this section, we provide a detailed analysis of the coverage provided by each technology and, consequently, the data rates achieved by the end-user. We have designed three scenarios which are based on the distance between the end-user and the WLAN and LTE access points. The user is always assumed to be in the same room, whereas the placement of WLAN and LTE access points varies with each scenario. For the VLC/WLAN network, when the AP is placed in the same room as the user, the end device achieved a fixed data rate of 183 Mbps in all cells. A comparison of VLC and WLAN data rates for the first scenario is shown in Figure 5 (a). In this scenario, the WLAN throughput is higher than that of the VLC by 80%. In the second scenario, the WLAN AP is placed in the opposite room and an average data rate of 149.01 Mbps is achieved with minimum and maximum values are observed as 147 Mbps and 150 Mbps, respectively. Comparison of the data rates of VLC and WLAN is presented in Figure 5 (b), where WLAN outperforms VLC by 71%. In the last scenario, the distance between the user and the AP is maximized in

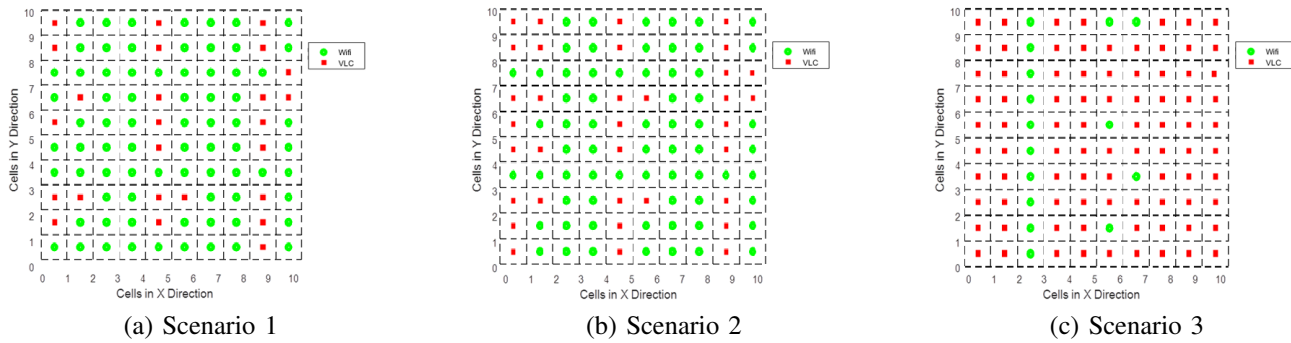


Fig. 5: 802.11ac access point and VLC connections as seen by the end user in three different scenarios

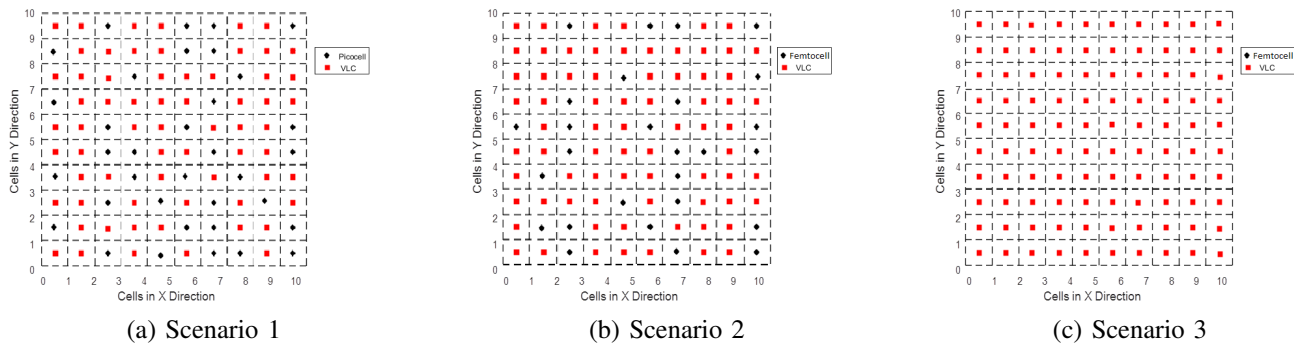


Fig. 6: LTE FBS and VLC connections as seen by the end user in three different scenarios

this case signal strength decreases around the edges of the room and eventually, the wireless connection between the user and the AP is lost. In this scenario, an average data rate of 60.1 Mbps is achieved with minimum and maximum values are respectively observed as 0 Mbps and 120 Mbps. In 27 cells, the signal strength was not strong enough to establish a connection between WLAN and the end-user. Comparison of the data rates of VLC and WLAN is presented in Figure 5 (c). In this scenario, the performance of VLC is better than WLAN by 79%.

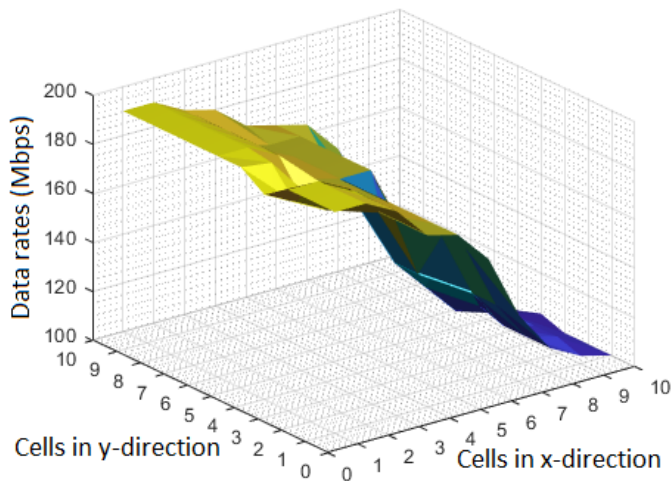
We further our investigation by recreating the same simulation environment, but this time with LTE FBS. In the first scenario, a constant data rate of 100 Mbps is achieved by the FBS. A comparison of VLC and LTE data rates is shown in Figure 6 (a). In this scenario, the throughput of LTE is higher as compared to the throughput of VLC in 34 cells. In the second scenario, the minimum and maximum values are achieved as 65 Mbps and 70 Mbps, respectively. A comparison of VLC and LTE data rates is shown in Figure 6 (b) evidencing that the performance of VLC is better in 72 cells. In the third case the user is not within the coverage area of femtocell and can not establish a connection. Therefore, it will be served by VLC as the user moves through the grid points, Figure 6 (c). Figure 6 shows the WLAN and FBS data rates as seen by the end user averaged over the three scenarios.

V. CONCLUSIONS

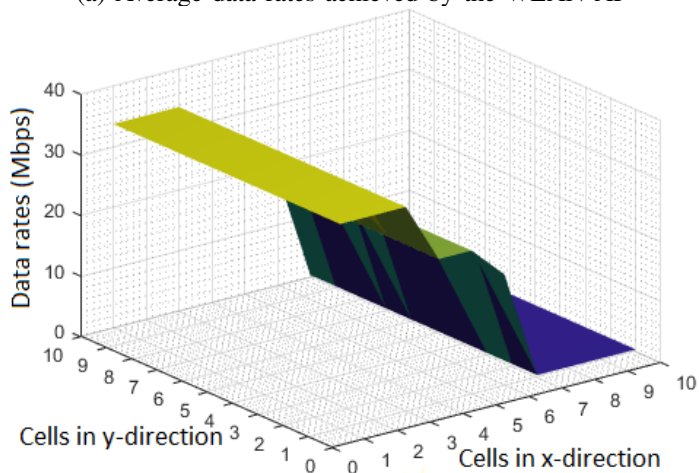
In this work, we investigated the combined utilization of VLC, WLAN, and LTE for the extension of coverage in an indoor environment. The aim of our work is to propose a solution that would provide connection to the end-users while maximizing the throughput. We considered an indoor apartment layout for the simulation environment and investigated the effect of user mobility on the achieved data rates. We show that in a homogenous network, the end-user experiences a degraded performance and even signal loss in some worst scenarios. Therefore, it can be concluded that as the demand for higher data rates and enhanced connection rises, a location-aware heterogeneous network of VLC with either WLAN or LTE is a viable solution.

REFERENCES

- [1] M. Ayyash et al. "Coexistence of WiFi and LiFi toward 5G: concepts, opportunities, and challenges". In: *IEEE Communications Magazine* 54.2 (2016), pp. 64–71.
- [2] F. M. Abinader et al. "Enabling the coexistence of LTE and Wi-Fi in unlicensed bands". In: *IEEE Communications Magazine* 52.11 (2014), pp. 54–61.
- [3] Sihua Shao et al. "Design and analysis of a visible-light-communication enhanced WiFi system". In: *Journal of Optical Communications and Networking* 7.10 (2015), pp. 960–973.



(a) Average data rates achieved by the WLAN AP



(b) Average data rates achieved by the FBS

Fig. 7: Data rates achieved by WLAN and Femtocell, averaged over the three scenarios

- [4] Arooba Zeshan and Tuncer Baykas. “Performance Analysis of VLC Based on 802.11 ac Frame Structure”. In: *IEEE Communications Letters* 23.9 (2019), pp. 1560–1563.
- [5] Helal Chowdhury, Ikram Ashraf, and Marcos Katz. “Energy-efficient connectivity in hybrid radio-optical wireless systems”. In: *ISWCS 2013; The Tenth International Symposium on Wireless Communication Systems*. VDE. 2013, pp. 1–5.
- [6] Lu Li, Hui Tian, and Bo Fan. “A joint resources allocation approach for hybrid visible light communication and LTE system”. In: (2015).
- [7] Shufei Liang et al. “A novel vertical handover algorithm in a hybrid visible light communication and LTE system”. In: *2015 IEEE 82nd Vehicular Technology Conference (VTC2015-Fall)*. IEEE. 2015, pp. 1–5.

- [8] E. Sarbazi et al. “Ray tracing based channel modeling for visible light communications”. In: *2014 22nd Signal Processing and Communications Applications Conference (SIU)*. Apr. 2014, pp. 702–705. DOI: 10.1109/SIU.2014.6830326.
- [9] George R Maccartney et al. “Indoor office wideband millimeter-wave propagation measurements and channel models at 28 and 73 GHz for ultra-dense 5G wireless networks”. In: *IEEE access* 3 (2015), pp. 2388–2424.
- [10] Scott Y Seidel and Theodore S Rappaport. “914 MHz path loss prediction models for indoor wireless communications in multifloored buildings”. In: *IEEE transactions on Antennas and Propagation* 40.2 (1992), pp. 207–217.
- [11] Scott Y Seidel and Theodore S Rappaport. “Site-specific propagation prediction for wireless in-building personal communication system design”. In: *IEEE transactions on Vehicular Technology* 43.4 (1994), pp. 879–891.
- [12] John S Seybold. *Introduction to RF propagation*. John Wiley & Sons, 2005.
- [13] A. J. Motley and J. M. P. Keenan. “Personal communication radio coverage in buildings at 900 MHz and 1700 MHz”. In: *Electronics Letters* 24.12 (June 1988), pp. 763–764. ISSN: 0013-5194. DOI: 10.1049/el:19880515.
- [14] Richard Watson. *Fixed/mobile convergence and beyond: unbounded mobile communications*. Newnes, 2008.
- [15] Jie Zhang and Guillaume De la Roche. *Femtocells: technologies and deployment*. John Wiley & Sons, 2011.
- [16] Holger Claussen, Lester TW Ho, and Louis G Samuel. “Self-optimization of coverage for femtocell deployments”. In: *2008 Wireless Telecommunications Symposium*. IEEE. 2008, pp. 278–285.